Soluble silicon nanoparticles–polyaniline capsules for biosensing and imaging

Noha Elhalawany
Polymers and Pigments Department, Chemical Industrial Division, National Research Center, Cairo 12311, Egypt

Yulia Maximenko
Department of Physics, University of Illinois at Urbana-Champaign, Urbana, Illinois 61801

Zain Yamani
Center of Excellence for Nanotechnology, KFUPM, Dhahran 31261, Saudi Arabia

Siu-Tung Yau
Department of Electrical Engineering, Cleveland State University, Cleveland, Ohio 44115

Munir H. Nayfeh[a)]
Department of Physics, University of Illinois at Urbana-Champaign, Urbana, Illinois 61801

(Received 5 June 2012; accepted 14 September 2012)

We used miniemulsion to synthesize novel water-soluble dispersion of nanocapsules with a polyaniline (PANI) shell and luminescent ultrasmall Si nanoparticle core with diameters of 50–300 nm. The capsules are functionalized with aromatic sulfonic acid. The capsules may be reconstituted in thin films or structured surfaces. The stability of the luminescence and dispersion of the capsules is studied under a wide range of pH conditions. The multiplicity of nanoparticles in the core provides highly amplified and reproducible signal for luminescence-based imaging using standard fluorescence microscopy, while the PANI shell allows a variety of routes for functionalization as well as electrical interrogation, which enables a wide range of biosensing/imaging applications.

I. INTRODUCTION

Biosensing and biomedicine using silicon-based nanomaterial are the active areas of research.[1–5] The active material includes Si nanoparticles, porous silicon, mesoporous Si oxide, as well as nanostructured Si compounds. We have recently produced novel ultrasmall Si nanoparticles with strong optical properties.[6–10] In the procedure, we disperse electrochemical etched Si into a discrete set of ultrasmall Si nanoparticles of diameter in the range of 1–3 nm, the smallest of which is of diameter 1 nm, comprising 29 Si atoms and is luminescent in the blue part of the spectrum. Unlike the bulk precursor, the particles have exquisite characteristics including being ultrabright[8] and nonlinear optical effects, including stimulated emission and harmonic generation.[9,10] Additionally, they exhibit strong catalytic properties, which were used to construct an amperometric sensor for substances of biomedical importance such as glucose.[11–13] The particles show good photostability under intense infrared as well as ultraviolet (UV) excitation.[14] The emission from single particles is readily detectable.[8] Such properties promise ultrasensitive Si-based sensing and imaging for biomedical applications. However, the detection of single particle requires the use of high peak power laser radiation. Moreover, the particles, especially the larger red luminescent particles, suffer from reduced solubility and stability in aqueous media. To alleviate these problems, we previously immobilized the Si nanoparticles on glass fiber carpets or pads, which consist of thousands of fibers to impart optical and chemical functions to thousands of fibers in parallel, enhancing the detection sensitivity and the sampled volume. Using the pads, we demonstrated the ability to detect substances such as amines.[15]

In this paper, we report on synthesis of novel water-soluble dispersion of nanocapsules with a polyaniline (PANI) shell and luminescent Si nanoparticles core with diameters of 50–300 nm. The multiplicity of luminescent nanoparticles in the core allows high sensitivity sensing and detection of a few capsules using standard fluorescence microscopy and, hence, provides highly amplified and reproducible signal for luminescence-based imaging and communication.

II. EXPERIMENTAL PROCEDURES

The Si nanoparticles are produced by chemical etching of single-crystal Si wafers in HF and H_2O_2 while charging the surface with an electric current[6] or by using hexachloroplatinic acid catalyst.[7] After the treatment, the wafers are sonicated in a liquid of choice to shake off a discrete set of ultrasmall Si nanoparticles of diameter in the range 1–3 nm.

[a)]Address all correspondence to this author.
e-mail: m-nayfeh@illinois.edu
DOI: 10.1557/jmr.2012.325

 © Materials Research Society 2012

https://doi.org/10.1557/jmr.2012.325 Published online by Cambridge University Press

The nanoparticles stay in suspension for easy recovery and reuse. The catalyst procedure predominantly produces red luminescent particles of 2.9 nm diameter. In the procedures, particles come out with a Si–H termination, which is a key to Si chemistry, enabling a variety of chemical routes for attachment with hydrocarbons.[16,17] Figure 1(a) gives a transmission electron microscope (TEM) image of the 2.9-nm particles on a graphite grid. Figure 1(b) gives the typical luminescence spectrum of the red particles in isopropyl alcohol (IPA), under UV excitation from an incoherent Hg lamp at a wave length of 365 nm.

We used a single-step miniemulsion procedure to encapsulate Si nanoparticles in PANI. We used dodecylbenzene sulfonic acid (DBSA), which is an anionic surfactant that has strong repulsive electrostatic polar groups. It is a protonic acid functionalized by dodecylbenzene, which is a benzene ring with a long chain of carbon. It has the property of detergency, moistening, foaming, emulsion, and dispersion. It can be directly used in producing all kinds of industrial and daily detergent. The biological degradability of DBSA is more than 90%. At the start of the polymerizing encapsulation process, DBSA dissolved in water–IPA mixture is homogenized with aniline at 10,000 rpm for 5 min to form a miniemulsion. We then add Si nanoparticles dispersed in IPA and ammonium peroxydisulfate (APS) as an initiator and repeat the homogenization for 12 min. Before polymerization, a mixture of aniline and Si nanoparticles is transparent in room light and shows the characteristic red emission from the nanoparticles under UV irradiation. The overall polymerization process resulted in a colloid, which exhibits a homogeneous light green in room light, characteristic of the color of PANI polymer in emeraldine state, and the characteristic red luminescence of the Si nanoparticles under UV.

In the encapsulation process, a solubilized anilinium salt, which acts as an emulsifier, forms and surrounds the Si particles. Macroradicals, which form by the homogenized degradation of aniline in presence of APS, are trapped by the Si particles, which in turn work as grafting sites allowing the grafting polymerization of aniline onto them leading to chemically stable dispersed PANI capsules with a luminescent center as shown schematically in Fig. 2(a). Also, PANI becomes protonated at the N sites, and the head of negative sulfonate ion ionically attaches to them as shown in Fig. 2(b). The sulfonate multiple oxygen atoms allow particles to dissolve in water though hydrogen bonding, while their long hydrophobic tails allow particles to dissolve in nonpolar solvents. PANI itself has attracted special interest because it has excellent electrical, electrochemical, and optical properties with applications in secondary batteries, electroluminescent devices, electrochromic devices, sensors, etc.[18] Unfunctionalized PANI, however, suffers from lack of solubility in aqueous media, and the use of DBSA was first reported as a means to make bulk PANI soluble in water.[19,20] Synthesis of colloidal dispersions[20,21] by chemical polymerization of aniline in the presence of different polymeric steric stabilizers[21–27] has helped alleviate solubility problems.

III. RESULTS AND DISCUSSION

A thin film of the capsules was formed on a device quality Si wafer by dispensing some volume of the capsule colloid on the wafer. The sample was left to dry under ambient conditions and was observed with a scanning electron microscope (SEM). Figure 3 shows the capsules being spherical of diameter in the range 100–300 nm. Few capsules can be seen of the order of 500 nm. In general, the capsule size can vary from 50 nm to several micrometers, which can be to some extent controlled by the fraction of aniline used in the encapsulation process.

We also examined the optical activity of capsules using fluorescence microscopy. Figure 4(a) gives the fluorescent images of capsules placed on a Si substrate using radiation at three wave lengths: 365, 480, and 550 nm. Under excitation at 550 nm (the absorption edge—the onset of the confinement band gap of the Si nanoparticles), the image shows red luminescence from the Si nanoparticles core and some scattered green light caused by PANI in its emeraldine state. Under excitation with radiation of wave length of 480–510 nm, the same structure appears mostly

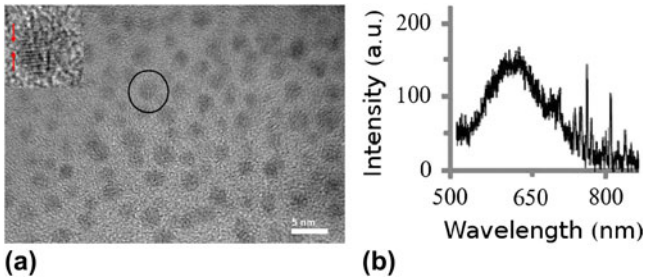


FIG. 1. (a) TEM image of the Si nanoparticles placed on a graphite grid. The inset is a magnified image of the circled particle showing the characteristic atomic planes of silicon. (b) Luminescence spectrum of a colloid of the particles in IPA using UV radiation at a wave length of 365 nm.

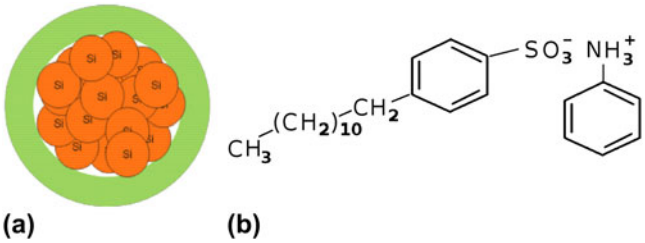


FIG. 2. (a) Schematic of a capsule showing a red luminescent core of Si nanoparticles under UV and a green jacket (shell) of PANI under white light. (b) Schematic of attachment of sulfonic acid ion with the PANI jacket.

https://doi.org/10.1557/jmr.2012.325 Published online by Cambridge University Press

green due to the PANI shell and lack of activity of Si nanoparticles in this range. Under excitation with UV radiation, the Si nanoparticles are strongly luminescent in the red range, while PANI may produce weak light blue. Depending on the thickness of the PANI shell, the capsule emission may have different shades of red.

We filtered the capsule colloid with a 1-μm paper filter. Some of the larger capsules in the distribution (of ≥300 nm) as well clusters of capsules were retained on the filter, while the smaller ≤300 nm capsules passed through the filter. The capsules on the filters, i.e., larger capsules, were redissolved in IPA for storage and delivery. We dispensed a certain volume of this colloid on device quality Si wafers. We imaged several random windows of 250 μm across using a fluorescence microscope, an example of which is shown in Fig. 5(a). We obtained the brightness (red channel) and spot size of structures. A single average brightness value was assigned to each spot by performing a measurement across the spot. We cast the spot parameters (brightness versus spot size) in Fig. 5(b). As seen in the figure, the smaller spots in the ensemble, namely 0.7 μm which is near the limit of resolution of the microscope, have the most uniform brightness. For larger spots, the brightness is more scattered and, on the average, is larger than that for smaller size structures. A histogram of the frequency of spots versus brightness is cast in Fig. 5(c). For capsules of identical luminescent core (identical capsules) and nonclustering, the brightness distribution would be sharp. The departure, namely scattered and wide distribution, arises from variation of core size, three-dimensional clustering (multiple layers), as well as lack of resolution. Taking 23–26 counts for the average contribution of a single capsule, the histograms show the domination of a single layer. The spot frequency in this case is decreasing with brightness, or, in other words, with the number of layers in the cluster (up to ~5–7 capsule layers). The above results show potential capability of detecting a few capsules down to 1–3 using standard fluorescence microscopy.

Smaller capsules that passed through the filter were recovered. We used transmission electron microscopy to image the smallest nanocapsules. A graphite grid was immersed in the colloid and imaged. We isolated in Fig. 6 a number of structures for illustration. The structures appear to consist of a dark core, which is associated with a silicon core, surrounded by a lighter density shell, which is associated with the polymer. The green and red colors observed with the fluorescence microscope (see Fig. 4) are produced by the light PANI shell and the dark Si core, respectively, in this structure. The diameter of the capsules is ~50 nm. The Si core is estimated to be ~20 nm in diameter, corresponding to a Si nanoparticles cluster of ~100–200 nanoparticles (each of a diameter of ~3 nm). The thickness of the polymer shell is estimated to be ~15 nm. Such capsules, at the smallest end of the size range, could not be observed with the standard fluorescence microscope. Previously, we detected emission from single silicon nanoparticles 1–3 nm in diameter using two-photon autocorrelation spectroscopy utilizing femtosecond pulses at a wave length of 780 nm.[8] The present results could lead to detection of the larger single capsules using simply a standard fluorescence microscope.

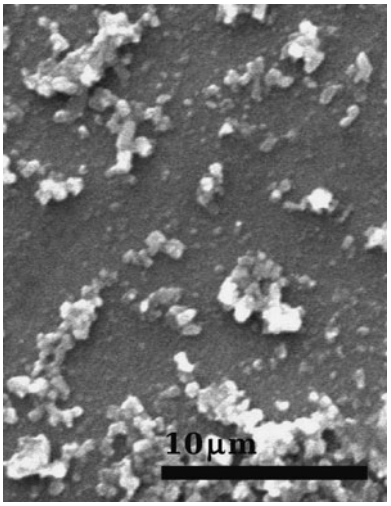


FIG. 3. SEM images of the capsules dispensed from the colloid and dried under ambient conditions on a Si wafer. It shows spherical particles of diameter in the range as small as 100–300 nm.

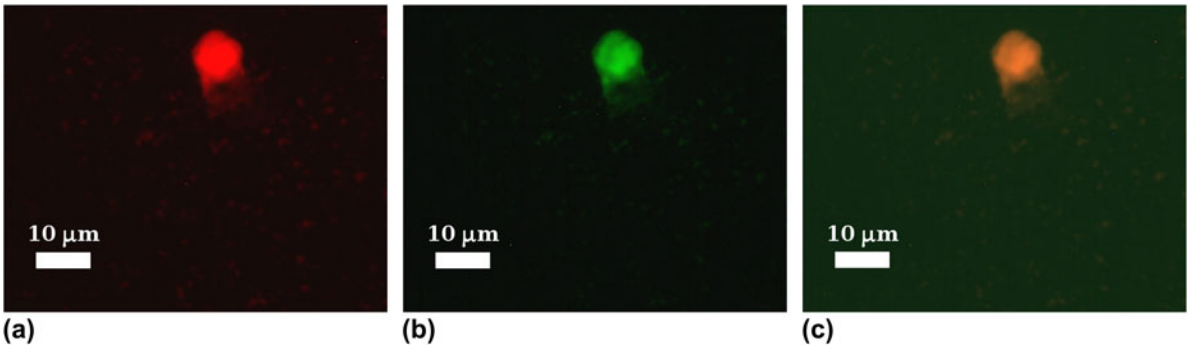


FIG. 4. Luminescent images using a fluorescence microscope of capsules on a Si wafer using wave lengths at (a) 365 nm, (b) 480 nm, and (c) 550 nm.

https://doi.org/10.1557/jmr.2012.325 Published online by Cambridge University Press

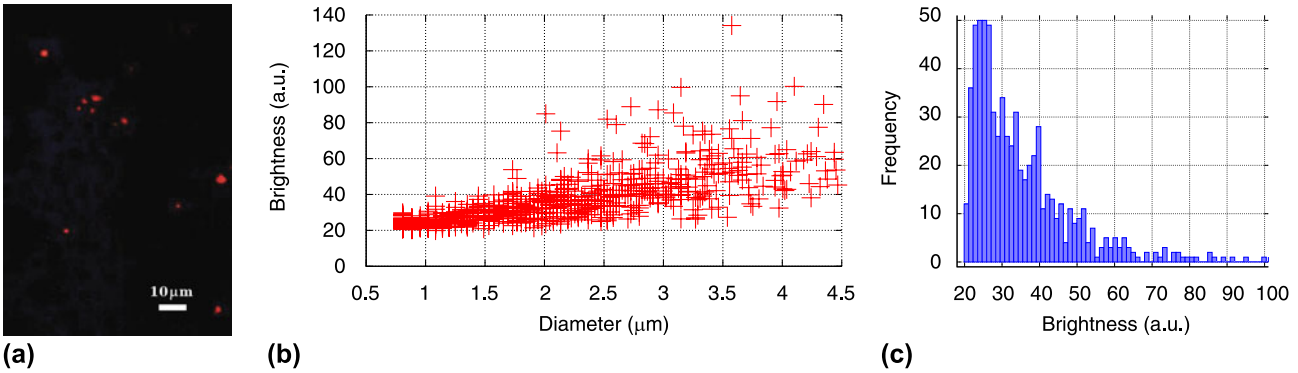


FIG. 5. (a) Luminescent image of capsules on a silicon wafer taken with a fluorescence microscope. (b) Brightness as a function of spot size for various structures. (c) Histogram of a spot frequency as a function of spot brightness.

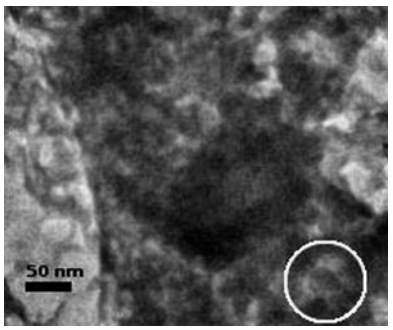


FIG. 6. High-resolution TEM image of a graphite grid dipped in a capsule colloid. The capsules appear to consist of a dark core, which may be associated with a Si core, surrounded by a lighter density jacket, which is associated with the polymer coating. An example of a capsule is circled in the image.

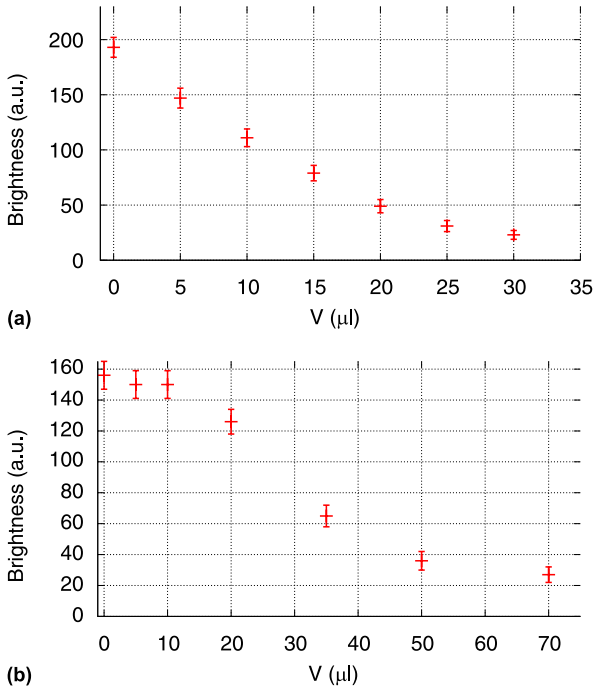


FIG. 7. Luminescence as a function of volume of a buffer added to (a) colloid of Si nanoparticles and (b) colloid of PANI–Si capsules.

The capsules are stable (luminescence and dispersion) in IPA. We have not observed a decrease in the optical activity over many months. In water, the capsules may deteriorate but they retain significant percentage of the luminescence over weeks. We examined the effect of pH environment on the stability of the luminescence and dispersion. As a reference, we first examined the effect on unencapsulated Si nanoparticles. Figure 7(a) gives the luminescence of a colloid of monodispersed Si nanoparticles as a function of the volume of the buffer added, which shows that buffer quenches the luminescence. The buffer used is a diluted with water pH 10 mixture of potassium carbonate, potassium borate, and potassium hydroxide buffer. Since the Si nanoparticles are synthesized with a Si–H termination, we believe that the buffer deprotonates the particles resulting in a radical (Si–H → Si–), which makes them highly reactive with the environment, in turn resulting in surface traps that quench the luminescence. pH readings over the range of buffer volume used in this experiment remain within the interval of 6.5–7 for particles–buffer mixture, which is equal to the pH value of pure particles in isopropanol. This observation confirms that particles react with buffer. On the other hand, measurements show that acids such as HCl do not quench the luminescence of the pure Si nanoparticles. In fact, upon adding a 1 M HCl to Si nanoparticles colloid in isopropanol, resulting in a pH drop from 6.5 to 1, the average brightness was measured at a level of 210 arbitrary counts compared to the initial brightness of 200 (luminescence images not shown). The stability is due to the fact that presence of HCl maintains the hydrogen termination of the particles.

Figure 7(b) gives the luminescence of a capsule colloid as a function of the volume of buffer added to a certain volume of capsules in isopropanol. Initially, the luminescence is stable; then, it begins to drop exponentially. Accompanied with the introduction of buffer, we observe some aggregation. It seems that the buffer deprotonates the PANI shell, resulting in the release of the sulfonate ion, which is

https://doi.org/10.1557/jmr.2012.325 Published online by Cambridge University Press

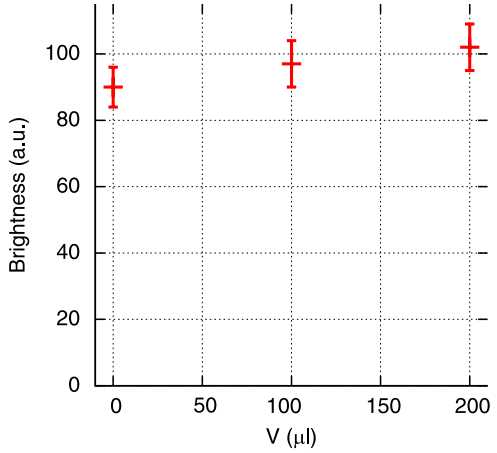


FIG. 8. Luminescence as a function of volume of 1 M HCl added to colloid of PANI–Si capsules. Brightness is normalized by volume due to the high volume ratio of added solution to initial solution.

electrostatically attached to the protonated site of the PANI shell (see Fig. 2), hence loss of solubility and emergence of aggregation. In the initial flat region, the amount of buffer is not enough to fully deprotonate the PANI shell. We believe that in the quenching regime, the buffer deprotonates the shell and begins to deprotonate the Si nanoparticles in the core, causing quenching of the luminescence, as discussed above. This deprotonation process is plausible because we observe that the pH of the colloid does not show the rise expected with the addition of the buffer and remains in the interval 6.5–7. In fact, when the same amount of buffer is added to a water control sample, the pH rise is noticeable with the same measuring device. This is consistent with the fact that the deprotonation of the PANI or particles neutralizes buffer, reducing the expected rise in pH. The conclusion is also supported by the fact that when acid solution is added to capsules, no quenching of the luminescence takes place (Fig. 8), while a significant pH drop from 6.5 to 1 is observed. The presence of an excessive amount of H^+ ions does not deprotonate the structures, i.e., no change in the chemical state of capsules and the core particles, thus the luminescence is maintained.

IV. CONCLUSION

In conclusion, we synthesized novel water-soluble dispersion of nanocapsules with a PANI shell and luminescent ultrasmall Si nanoparticles core with diameters of about 50–300 nm. Clusters of a small number of capsules are observable with a standard fluorescence microscope. The capsules exhibit photostability in acidic and limited basic environments. The ongoing research is focusing on replacing the sulfonate termination with other molecules that are covalently attached to the PANI shell to establish robust stability in a wider range of pH environment including a base environment. The PANI shell allows routes for functionalization as well as electrical interrogation. The capsules may also constitute a good sensitizer material for photovoltaic solar cell application.

ACKNOWLEDGMENT

The authors acknowledge NSF Grant OISE 11-03-398.

REFERENCES

1. Y. He, C. Fan, and S-T. Lee: Silicon nanostructures for bioapplications. *Nanotoday* **5**, 282 (2010).
2. F. Erogbogbo, K-T. Yong, I. Roy, G. Xu, P.N. Prasad, and M.T. Swihart: Biocompatible luminescent silicon quantum dots for imaging of cancer cells. *ACS Nano* **2**, 873 (2008).
3. M.H. Nayfeh and L. Mitas: Silicon nanoparticles: New photonic and electronic material at the transition between solid and molecule, in *Nanosilicon*, edited by V. Kumar (Elsevier, Amsterdam, The Netherlands, 2008); pp. 1–78.
4. D.S. English, L.E. Pell, Z. Yu, P.F. Barbara, and B.A. Korgel: Size tunable visible luminescence from individual organic monolayer stabilized silicon nanocrystal quantum dots. *Nano Lett.* **2**, 681 (2002).
5. M. Nayfeh, E. Rogozhina, and L. Mitas: Silicon nanoparticles: Next generation of ultrasensitive fluorescent markers, in *Synthesis, Functionalization, and Surface Treatment of Nanoparticles*, edited by M.-I. Baratron (American Scientific Publishers, Stevenson Ranch, CA, 2002); pp. 1–59.
6. G. Belomoin, J. Therrien, A. Smith, S. Rao, S. Chaieb, and M.H. Nayfeh: Observation of a magic discrete family of ultrabright Si nanoparticles. *Appl. Phys. Lett.* **80**, 841 (2002).
7. D. Nielsen, L. Abuhassan, M. Alchihabi, A. Al-Muhanna, J. Host, and M.H. Nayfeh: Current-less anodization of intrinsic silicon powder grains: Formation of fluorescent Si nanoparticles. *J. Appl. Phys.* **101**, 114302 (2007).
8. O. Ackakir, J. Therrien, G. Belomoin, N. Barry, J. Muller, E. Gratton, and M.H. Nayfeh: Detection of luminescent single ultrasmall silicon nanoparticle using fluctuation spectroscopy. *Appl. Phys. Lett.* **76**, 1857 (2000).
9. M.H. Nayfeh, J. Therrien, G. Belomoin, O. Akcakir, N. Barry, and E. Gratton: Stimulated blue emission and second harmonic generation from films of ultrasmall Si nanoparticles, in *Microcrystalline and Nanocrystalline Semiconductors—2000*, edited by P.M. Fauchet, J.M. Buriak, L.T. Canham, N. Koshida, and B.E. White, Jr. (Mater. Res. Soc. Symp. Proc. **638**, Warrendale, PA, 2001); p. F9.5.
10. M. Nayfeh, O. Akcakir, G. Belomoin, N. Barry, J. Therrien, and E. Gratton: Second harmonic generation in microcrystallite films of ultrasmall Si nanoparticles. *Appl. Phys. Lett.* **77**, 4086 (2000).
11. G. Wang, K. Mantey, M.H. Nayfeh, and S-T. Yau: Enhanced amperometric detection of glucose using Si-29 particles. *Appl. Phys. Lett.* **89**, 243901 (2006).
12. G. Wang, S-T. Yau, K. Mantey, and M.H. Nayfeh: Fluorescent Si nanoparticle-based electrode for sensing biomedical substances. *Opt. Commun.* **281**, 1765 (2008).
13. Q. Liu, M.H. Nayfeh, and S-T. Yau: A silicon nanoparticle-based polymeric nano-composite material for glucose sensing. *J. Electroanal. Chem.* **657**, 172 (2011).
14. K. Mantey, M. Kwit, M.H. Nayfeh, A. Kumar, L.D. Stephenson, and A.J. Nelson: Measurement of the photostability of silicon nanoparticles under UVA and near infrared irradiation. *J. Appl. Phys.* **107**, 064316 (2010).
15. K. Mantey, M.H. Nayfeh, B. Al-Hreish, J. Boparai, A. Kumar, L.D. Stephenson, A.J. Nelson, S.A. Alrokayan, and K.M. Abu-Salah: Silicon nanoparticle-functionalized fiberglass pads for sampling. *J. Appl. Phys.* **109**, 064321 (2011).

https://doi.org/10.1557/jmr.2012.325 Published online by Cambridge University Press

16. E. Rogozhina, G. Belomoin, A. Smith, L. Abuhassan, N. Barry, O. Akcakir, P.V. Braun, and M.H. Nayfeh: Si-N linkage in ultrabright, ultrasmall Si nanoparticles. *Appl. Phys. Lett.* **78**, 3711 (2001).
17. G. Belomoin, E. Rogozhina, J. Therrien, P.V. Braun, L. Abuhassan, M.H. Nayfeh, L. Wagner, and L. Mitas: Effect of surface termination on the band gap of ultrabright Si_{29} nanoparticles: Experiments and computational models. *Phys. Rev. B* **65**, 193406 (2002).
18. A.J. Heeger: Semiconducting metallic polymers: Fourth generation polymeric materials. *Angew. Chem. Int. Ed.* **40**, 2591 (2001).
19. A.G. Green and A.E. Woodhead: Aniline black and allied compounds. *J. Chem. Soc.* **97**, 2388 (1910).
20. A.A. Syed and M.K. Dinesan: Polyaniline-A novel polymeric material. *Talanta* **38**, 815 (1991).
21. P. Banerjee: Carboxymethylcellulose stabilized polyaniline dispersions and conducting copolymer latex composites. *Eur. Polym. J.* **34**, 841 (1998).
22. D. Chattopadhyay and B.M. Mandal: Methyl cellulose stabilized polyaniline dispersions. *Langmuir* **12**, 1585 (1996).
23. J. Stejskal and P. Kratochvil: Polyaniline dispersions. 5. Poly(vinyl alcohol) and poly(N-vinylpyrrolidone) as steric stabilizers. *Langmuir* **12**, 3389 (1996).
24. P. Banerjee, S.N. Bhattacharyya, and B.M. Mandal: Poly(vinyl methyl-ether) stabilized colloidal polyaniline dispersions. *Langmuir* **11**, 2414 (1995).
25. E.C. Cooper and B. Vincent: Electrically conducting organic films and beads based on conducting latex particles. *J. Phys. D: Appl. Phys.* **22**, 1580 (1989).
26. S.P. Armes, M. Aldissi, S. Agnew, and S. Gottesfeld: Aqueous colloidal dispersions of polyaniline formed by using poly(vinylpyridine)-based steric stabilizers. *Langmuir* **6**, 1745 (1990).
27. S.H. Lee, D.H. Lee, K. Lee, and C.W. Lee: High-performance polyaniline prepared via polymerization in a self-stabilized dispersion. *Adv. Funct. Mater.* **15**, 1495 (2005).

https://doi.org/10.1557/jmr.2012.325 Published online by Cambridge University Press